JCAMECH

Vol. 51, No. 2, December 2020, pp 374-388
DOI: 10.22059/jcamech.2020.303046.510

Free vibration behavior of bi-directional functionally graded plates with porosities using a refined first order shear deformation theory

B. Sidda Reddy[a,] ∗ K. Vijaya Kumar Reddy[b] and B. Chinna Ankanna[c]

[a,c] *Rajeev Gandhi Memorial College of Engineering & Technology, Nandyal, Kurnool, A.P, India*
[b] *Jawaharlal Nehru Technological University, Hyderabad, Telangana, India*

ARTICLE INFO

Article history:
Received: 18 May 2020
Accepted: 01 July 2020

Keywords:
Bidirectional Functionally graded plates
Porosities
Free vibration
Rule of Mixtures
Lagrange Equations

ABSTRACT

This paper proposes the refined first order shear deformation theory to investigate the free vibration behavior of bidirectional functionally graded porous plates. This theory satisfies the transverse shear stress free conditions at the top and bottom of the plate, thus avoids the need of a shear correction factor. The rule of mixtures is employed to compute the effective material properties and assumed to be graded in both x and z-directions. The equations of motion are derived by means of Lagrange equations to investigate the free vibration response. The displacement functions in axial and transverse directions are expressed in simple algebraic polynomial series form, including admissible functions which are used to fulfill the simply supported boundary conditions. The admissible functions are generated using Pascal's triangle. The accuracy of the present theory is assessed with the numerical results and is confirmed by comparing with 3-D exact solutions and with other higher order theories. The influence of thickness ratios, aspect ratios, gradation indexes, type of porosity distribution and the volume fraction of porosity on the free vibration behavior of bi-directional FGPs are discussed in detail. The presented numerical results can be used as benchmark solutions to assess the various plate theories and compare with solutions obtained by other analytical and finite element methods. From the present work, it can be concluded that the present theory allows examining the vibration behavior of bidirectional porous FG plates manufactured in the sintering process.

1. Introduction

Functionally graded materials (FGMs) are distinct engineering materials, fabricated by changing the properties in different directions continuously to yield specific characteristics that are significantly different from those of its constituents. FGMs are extensively used in several areas of engineering, because of their exceptional advantages, for instance, avoidance of failure due to delamination and stress concentration at the interface, lower thermal stress as structural components subjected to large temperature difference environments such as aircraft structures and cracking issues which can be found in laminated composites [1-3].

The functionally graded Plates (FGPs) are the key elements, widely used in numerous structural systems such as aircraft, automotive, space vehicles, civil, shipbuilding, chemical, energy sources, biomedical, optical and mechanical engineering [4-5]. In the past few decades, researchers have paid great attention to the investigation of the structural behavior of perfect FGPs [6-20], as well as porous FG structures [4-5, 21-32], just to name a few. The authors were used the first-order and higher order theories to define the kinematics of the plate. Zamani Nejad et al. [33] studied the elastic behavior of thick walled FG spherical pressure vessels under internal pressure using a semi-analytical iterative method. In this paper, the material properties varied exponentially in the thickness direction of the sphere. These authors [34] also investigated the ealsto-plastic deformations and stresses in FG rotating disk by employing the elasto-perfectly-plastic material model. The influence of angular speed of the propagation of the plastic zone was studied and concluded that the density variation had a significant effect on the variation of deformations and stresses.

Mohammad Hosseini et al. [35-37] adopted a strain gradient theory to analyze the stresses in a rotating functionally graded nano-disk subjected to thermo-mechanical loads by keeping the thickness as constant and varying nonlinearly. The thickness

* Corresponding author. Tel.: +91-9440-844-0600; fax: +91-851-427-5123; e-mail: bsrrgmcet@gmail.com

parameters had a larger effect compared to the graded index and the difference in stress estimated by classical theory and the strain gradient theory is large for the small thickness of the nano - disk. Zeinab Mazarei and Mohammad Zamani Nejad [38] analyzed the thick-walled functionally graded spherical vessel as thermo-elasto-plastic problem by assuming the inner and outer surface exposing to a uniform heat flux and an airstream respectively. The FG rotating thick cylindrical pressure vessels were analyzed for stresses by Mohammad Zamani Nejad et al. [39] using Frobenius series method under plane stress as well as plane strain conditions and compared with the finite element results. Mohammad Zamani Nejad et al. [40] presented a comprehensive literature review on the analysis of thick shells by elastic theories, shear deformation theories, simplified theories and mixed theories of functionally graded thick cylindrical and conical shells. Amin Hadi et al. [41] analyzed the influence of capture size in a spheroid living cell membrane under hydrostatic pressure using strain gradient theory. The stresses in rotating functionally graded cylindrical pressure vessels were evaluated by Nejad et al. [42] under thermal load for purely elastic, partially plastic and fully plastic deformation condition by assuming the inner surface exposed to an airstream and the outer surface exposed to a uniform heat flux.

Behrouz Karami et al. [43] investigated the resonance behavior of Kirchhoff-three directional FG nano-plates using a unified model. The bi-Helmholz nonlocal strain gradient theory considered to capture the influence of small scale. Esmail Zarezadeh et al. [44] studied the influence of capture size in functionally graded nano-rod under magnetic field supported by a torsional foundation using nonlocal elasticity theory. To define the influence of torque of an axial magnetic field Maxwell's relation has been used.

The cited papers [4-5, 21-44] constrained to change the material properties in only one particular direction. This may be futile in the design of components used in propulsion systems and space applications, which often subject to large temperature difference in more than one direction [45]. For this purpose, two-directional FGMs are introduced, which are of great importance in the design as well as development of various advanced engineering applications like space crafts and space shuttles, particularly where effective high heat resistant materials are essential. Hence, the development of bi-directional or multi-directional FGMs is essential and useful in the design of advanced structures. In view of this, bi-directional FGMs are presented in the literature briefly, e.g., see [45-67].

Nemat-Alla [45], developed two-directional FGMs and the numerical results shown that they have greater capability in reducing the thermal stresses compared to the one dimensional FGMs. The investigations pertaining to the bi-directional FGMs have been carried out recently and available in the open literature. For example, Nemat-Alla [46] optimized the material composition using a finite element model to reduce the temperature stresses of bi-directional FGMs which operate at a harsh temperature loading cycle using ZrO2/6061-T6/Ti-6Al-4V.

Asgari and Akhlaghi [47] developed the three dimensional elasticity equations, while Ebrahimi and Najafizadeh [48] applied the generalized differential quadrature and generalized integral quadrature methods to investigate the vibration behavior of bi-directional FG thick hollow cylinders.

Many research works were carried out on bi-directional FG Euler Bernoulli/Timoshenko as well as nano beams to investigate the nonlinear bending by Li et al [49], vibration behavior [50-54] or buckling analysis [55-56], just to name a few. Karamanli [57] used a quasi-3D shear deformation theory to study the bending behavior of bi-directional FG sandwich beams, while Lezgy-Nazargah [58] adopted NURBS based iso-geometric finite element method to investigate the thermo-mechanical behavior of 2-D FG beams.

As stated by Apalak and Demirbas in [59], the gradient exponents may not affect the temperature distributions, however, they affects significantly the heat transfer durations in bi-directional FGMs. Van Do et al. [60] used the third order shear deformation theory and finite element method to examine the bending, and buckling analysis of bi-directional FGPs. They concluded that obtaining the results for bi-directional FGPs are more complicated compared to unidirectional FGPs, because of gradation in two different directions.

Lieu et al. [61] investigated the bending and free vibration analysis of in-plane bi-directional FGPs considering the variable thickness using Iso-geometric analysis. The free vibration and buckling of in-plane bidirectional FGPs were also analyzed by Lieu et al. [62] by utilizing the non-uniform rational B-spline based material mesh and generalized shear deformation theory. Chen et al. [63] used the first order shear deformation theory in combination of iso-geometric analysis to study the natural vibration of sector cylindrical shells made of bi-directional FGMs with restrained edges. The dynamic analysis of bi-directional FGPs reinforced by eccentrically outside stiffeners under moving load with a constant velocity studied by Esmaeilzadeh and Kadkhodayan [64]. Abbas Barati et al. [65] investigated the bi-directional FG parameters, size-dependent parameter, and the value of the magnetic field on bi-directional functionally graded nanobeams under a longitudinal magnetic field of transverse vibrations. The small-scale influence exploited by the nonlocal elasticity theory. The effect of small scale on static torsion of the bidirectional FG Microtube was also investigated using the couple stress theory by Abbas Barati et al. [66] by changing the material properties along radius and length of tube. Noroozi et al. [67] used the nonlocal strain gradient theory to investigate the influence of size dependency of bidirectional FG nonlinear cone subjected to torsional vibration. The conclusion from their study is that the nonlocal elasticity theory behaves softer and strain gradient theory behaves harder.

The FGMs are fabricated in many ways; for example, multi-step sequential infiltration technique, non-pressure sintering technique, powder metallurgy, self-propagating high temperature synthesis technique and vapor deposition. However, in the production of the FGMs in the sintering process, porosities and micro voids may occur in the produced material. This is because of the metal phase coagulated at very high temperature and ceramic phase is at a relatively low temperature. The presence of pores will exotically weaken the strength of the material [68]. So, it is crucial to investigate the porosity effect in designing the bi-directional FGM components.

Based on the open source literature and to the author's knowledge, it is concluded that the analysis of bidirectional FGPs is complicated and needs to develop a simple and efficient theory which can predict the structural behavior of advanced structures accurately and also needs to consider the porosity effect.

The present paper is bestowed to develop a simple and refined first order shear deformation theory to investigate the free vibration behavior of bi-directional FGPs considering the porosities. The present refined first order theory involves only four unknowns, which is less than the number of unknowns (five) as in conventional first order theory and other higher order theories.

The present theory significantly reduces the computational efforts. The transverse displacement is divided into bending and shears parts. The polynomial type shape function is incorporated into the shear strain, which accounts the p^{th} order (p=3, 5, 7 …) variation of transverse shear strain along the thickness of the plate. This eliminates the need of a shear correction factor. The bi-directional FGP materials properties are assumed to change gradually in two directions (z-direction and x-direction) while the Poisson's ratio keeps on constant. The equations of motion are derived by means of Lagrange equations. The in-plane and transverse displacements are expressed in simple algebraic polynomial series form, including admissible functions which are used to fulfill the boundary conditions. The admissible functions are generated using Pascal's triangle. The accuracy of the present theory is assessed with the numerical results and is confirmed by comparing with 3-D exact solutions and with other higher order theories. The influence of thickness ratios, aspect ratios, gradation indexes, porosity distribution and the volume fraction of porosity on the free vibration behavior of bi-directional FGPs are discussed in detail.

2. Problem formulation

A bi-directional FG porous rectangular plate is assumed to be made up of three different materials. The physical dimensions of the plate are shown in Figure 1. The plate material properties, including modulus of elasticity and mass density vary both in the z-direction and in the x-direction. It is assumed that, the even porosity has porosities with even distribution of volume fraction over the cross section, while the uneven porosity has porosity spreading frequently near by the middle zone of the cross section and the amount of porosity seems to be linearly decreased at the top and bottom of the cross section. The effective modulus of elasticity and mass density changes according to the Eqs. (1-2).

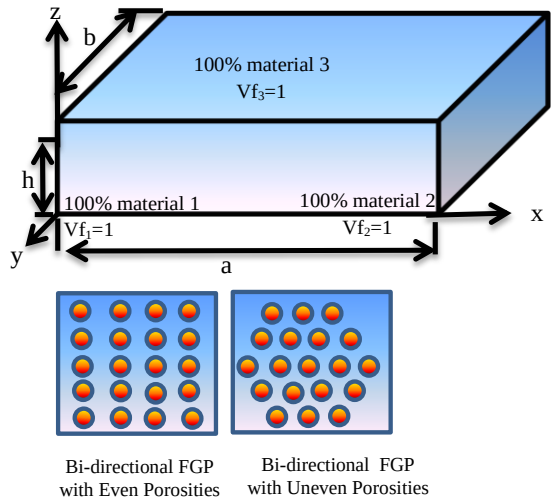

Figure.1. Representation of a bi-directional FGP with even and uneven porosity distributions

Even porosity model:

$$E(x,z) = E_1\left(1-\frac{x}{a}\right)^{\eta_1}\left(1-\left(\frac{z}{h}+\frac{1}{2}\right)^{\eta_2}\right)+E_2\left(\frac{x}{a}\right)^{\eta_1}\left(1-\left(\frac{z}{h}+\frac{1}{2}\right)^{\eta_2}\right)+E_3\left(\frac{z}{h}+\frac{1}{2}\right)^{\eta_2}-\frac{\gamma}{2}(E_1+E_2+E_3) \quad (1a)$$

$$\rho(x,z) = \rho_1\left(1-\frac{x}{a}\right)^{\eta_1}\left(1-\left(\frac{z}{h}+\frac{1}{2}\right)^{\eta_2}\right)+\rho_2\left(\frac{x}{a}\right)^{\eta_1}\left(1-\left(\frac{z}{h}+\frac{1}{2}\right)^{\eta_2}\right)+\rho_3\left(\frac{z}{h}+\frac{1}{2}\right)^{\eta_2}-\frac{\gamma}{2}(\rho_1+\rho_2+\rho_3) \quad (1b)$$

Uneven porosity model:

$$E(x,z) = E_1\left(1-\frac{x}{a}\right)^{\eta_1}\left(1-\left(\frac{z}{h}+\frac{1}{2}\right)^{\eta_2}\right)+E_2\left(\frac{x}{a}\right)^{\eta_1}\left(1-\left(\frac{z}{h}+\frac{1}{2}\right)^{\eta_2}\right)+E_3\left(\frac{z}{h}+\frac{1}{2}\right)^{\eta_2}-\frac{\gamma}{2}\left(1-\frac{2|z|}{h}\right)(E_1+E_2+E_3) \quad (2a)$$

$$\rho(x,z) = \rho_1\left(1-\frac{x}{a}\right)^{\eta_1}\left(1-\left(\frac{z}{h}+\frac{1}{2}\right)^{\eta_2}\right)+\rho_2\left(\frac{x}{a}\right)^{\eta_1}\left(1-\left(\frac{z}{h}+\frac{1}{2}\right)^{\eta_2}\right)+\rho_3\left(\frac{z}{h}+\frac{1}{2}\right)^{\eta_2}-\frac{\gamma}{2}\left(1-\frac{2|z|}{h}\right)(\rho_1+\rho_2+\rho_3) \quad (2b)$$

Where, E_1, E_2, E_3, and ρ_1, ρ_2, ρ_3 are modulus of elasticity and mass density of the three materials, respectively, while η_1 and η_2 are the *g*radation indexes along the x and z directions respectively, h is the thickness of the plate and γ is the volume fraction of porosity. $\gamma = 0$ represents the perfect bi-directional FG plate. The effective modulus of elasticity (E_{eff}) of bi-directional FGP depends upon the constituent material properties given in Table 1. The E_{eff} is determined by the Eqs. (1a, 2a) and is shown in Figures 2*a*-*b* for the specific case of $\eta_1 = 5, \eta_2 = 2$ thickness ratio, a/h=10 and $\gamma = 0, 0.1$ and 0.2 .

$$E_{eff} = \frac{\int_0^a \int_0^b \int_{-h/2}^{h/2} E(x,z)\,dz\,dy\,dx}{abh} \quad (3)$$

Table 1: Constituent material properties of bi-directional FGP [60, 73].

Properties of the material	Material-1	Material-2	Material3
E (GPa)	205.1	70	151
$\rho\ (kg/m^3)$	7813	2702	3000
μ	0.3	0.3	0.3

In addition, Figures 3*a* and *b* show the variation of effective modulus of elasticity, E(x, z) of porous bi-directional FG plate (from Eq. (3)). From Figures 3a and *b*, it is seen that the modulus of elasticity decreases with the increase of volume fraction of porosity and gradation index η_2, while it increases with η_1.

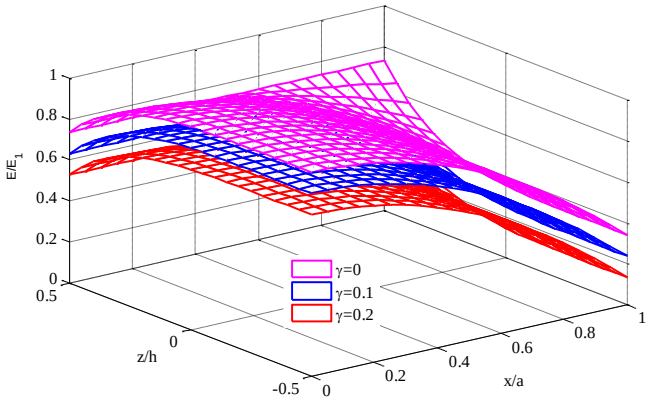

(a)

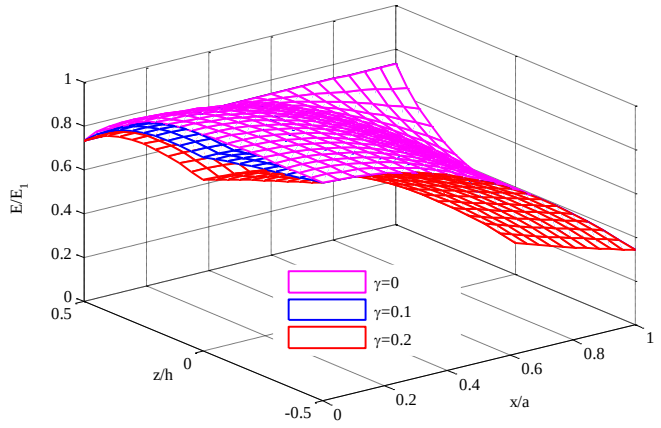

(b)

Figure. 2. The modulus of elasticity of porous bi-directional FGP (a) Even; (b) Uneven porosity distribution

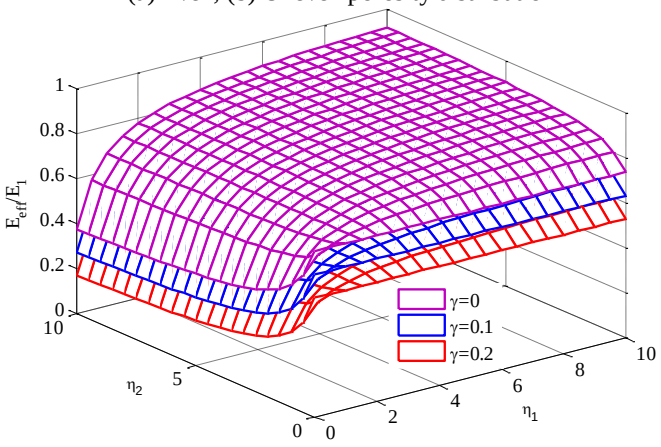

(a)

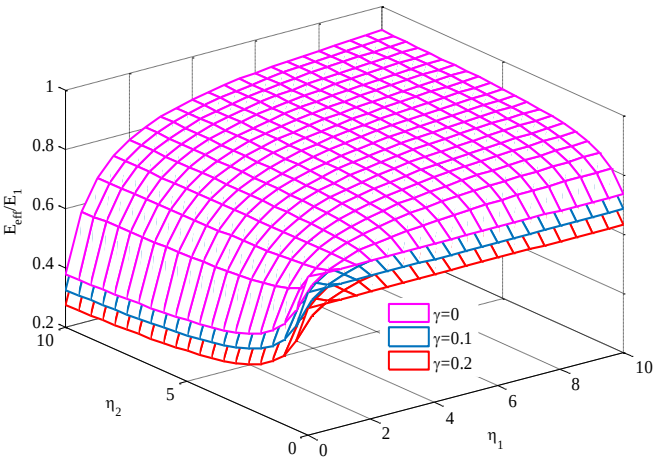

(b)

Figure. 3. Variation of modulus of Elasticity of the porous bi-directional FGP as a function of η_1, η_2 and γ; (a) Even (b) Uneven porosity distribution

2.1. Kinematic Relations

In the present refined first order shear deformation theory (RFSDT), the transverse displacement w is divided into bending (w_b) and shear (w_s) parts. The displacement field of the RFSDT can be written as

$$\bar{u}(x,y) = u - zw_{b,x} \tag{4a}$$
$$\bar{v}(x,y) = v - zw_{b,y} \tag{4b}$$
$$\bar{w} = w_b + w_s \tag{4c}$$

The comma followed by the subscripts is differentiation with respect to the subscripts throughout the paper. The RFSDT comprises only four unknown parameters.

2.2. Strain displacement relations

The strains associated with the displacement field of Eqns. (4a-c), can be given as.

$$\epsilon_x = u_{,x} - zw_{b,xx} \tag{5a}$$
$$\epsilon_y = v_{,y} - zw_{b,yy} \tag{5b}$$
$$\epsilon_{xy} = (u_{,y} + v_{,x}) - 2zw_{b,xy} \tag{5c}$$
$$\epsilon_{xz} = \left(1 - \left(\frac{2z}{h}\right)^{p-1}\right) w_{s,x} \tag{5d}$$
$$\epsilon_{yz} = \left(1 - \left(\frac{2z}{h}\right)^{p-1}\right) w_{s,y} \tag{5e}$$

The transverse shear strains are incorporated with the p^{th} order polynomial (p=3, 5, 7, 9….), which describes the variation of transverse shear strains through the thickness of the plate. Undoubtedly, the simple first order shear deformation theory was based on the assumption that the shear strain varies linearly across the thickness, so a shear correction factor was needed to avoid the shear locking phenomenon. Nevertheless, in the RFSDT, the shear strain was distributed with the p^{th} order of polynomial across the thickness and disappeared on the top and bottom of the plate. Thus, the present RFSDT avoids the need of a shear correction factor.

2.3. Stress-strain relations

The linear stress-strain relations for bi-directional FGPs are given as:

$$s_x = \frac{E(x,z)}{1-\mu^2}\epsilon_x + \frac{\mu E(x,z)}{1-\mu^2}\epsilon_y \tag{6a}$$
$$s_y = \frac{\mu E(x,z)}{1-\mu^2}\epsilon_x + \frac{E(x,z)}{1-\mu^2}\epsilon_y \tag{6b}$$
$$[s_{xy}\ s_{xz}\ s_{yz}] = \frac{E(x,z)}{2(1+\mu)}[\epsilon_{xy}\ \epsilon_{xz}\ \epsilon_{yz}] \tag{6c}$$

In which, $\{s_x, s_y, s_{xy}, s_{xz}, s_{yz}\}$ and $\{\epsilon_x, \epsilon_y, \epsilon_{xy}, \epsilon_{xz}, \epsilon_{yz}\}$ are the stresses and strains with regard to the plate coordinating system.

2.4. Free vibration problem formulation

The strain energy of the bi-directional FGP can be written as:

$$U = \frac{1}{2}\int_0^a \int_0^b \int_{-h/2}^{h/2} \left[s_x\epsilon_x + s_y\epsilon_y + s_{xy}\epsilon_{xy} + s_{xz}\epsilon_{xz} + s_{yz}\epsilon_{xz}\right] dzdydx \tag{7}$$

Substituting Eqns. (5-6) into Eq. (7), the strain energy can be taken as the form

$$U = \frac{1}{2}\int_0^a \int_0^b \int_{-h/2}^{h/2} \left[\frac{E(x,z)}{1-\mu^2}\left(u_{,x}{}^2 + z^2\left(w_{b,xx}{}^2 + w_{b,yy}{}^2\right) - 2z\left(u_{,x}w_{b,xx} + v_{,y}w_{b,yy}\right) + v_{,y}{}^2\right) + 2\mu\frac{E(x,z)}{1-\mu^2}\left(u_{,x}v_{,y} - z(v_{,y}w_{b,xx} + u_{,x}w_{b,yy}) + z^2 w_{b,xx}{}^2 w_{b,yy}{}^2\right) + \frac{E(x,z)}{2(1+\mu)}\left((u_{,y} + v_{,x})^2 - 4z(u_{,y} + v_{,x})w_{b,xy} + 4z^2 w_{b,xy}{}^2 + \left(1 - \left(\frac{2z}{h}\right)^{p-1}\right)^2 (w_{s,x}{}^2 + w_{s,y}{}^2)\right)\right] dzdydx \tag{8}$$

Similarly the kinetic energy of the bi-directional FGP can be written as:

$$K = \frac{1}{2}\int_0^a \int_0^b \int_{-h/2}^{h/2} \rho\left[\bar{u}_{,t}{}^2 + \bar{v}_{,t}{}^2 + \bar{w}_{,t}{}^2\right] dzdydx \tag{9}$$

Substituting the kinematic relations Eq. (4) into Eq. (9), kinetic energy can be written as

$$K = \frac{1}{2}\int_0^a \int_0^b \int_{-h/2}^{h/2} \rho\left[{u_{,t}}^2 + {v_{,t}}^2 + z^2\left({w_{b,xt}}^2 + {w_{b,yt}}^2\right) - 2zu_{,t}\, w_{b,xt} - 2zv_{,t}\, w_{b,yt} + {w_{b,t}}^2 + {w_{s,t}}^2 + 2w_{b,t}w_{s,t}\right] dzdydx \quad (10)$$

It is acknowledged that Hamilton's principle can be articulated as Lagrange equations, when displacement functions can be expressed in generalized coordinates [69]. Thus, the in-plane and transverse displacement functions $u(x, y)$, $v(x, y)$, $w_b(x, y)$, and w_s (x, y) are denoted by the following polynomial series which satisfies the kinematic boundary conditions.

$$u(x,y,t) = u_i\psi_i(x,y)e^{i\omega t},$$
$$\psi_i(x,y) = x^{p_u}y^{q_u}(x-a)^{r_u}(y-b)^{s_u}{\phi_i}^u(x,y) \quad (11a)$$
$$v(x,y,t) = v_i\lambda_i(x,y)e^{i\omega t},$$
$$\lambda_i(x,y) = x^{p_v}y^{q_v}(x-a)^{r_v}(y-b)^{s_v}{\phi_i}^v(x,y) \quad (11b)$$
$$w_b(x,y,t) = {w_b}_i\Delta_i(x,y)e^{i\omega t},$$
$$\Delta_i(x,y) = x^{p_{w_b}}y^{q_{w_b}}(x-a)^{r_{w_b}}(y-b)^{s_{w_b}}{\phi_i}^{w_b}(x,y) \quad (11c)$$
$$w_s(x,y,t) = {w_s}_i\Omega_i(x,y)e^{i\omega t},$$
$$\Omega_i(x,y) = x^{p_{w_s}}y^{q_{w_s}}(x-a)^{r_{w_s}}(y-b)^{s_{w_s}}{\phi_i}^{w_s}(x,y) \quad (11d)$$

Where $u_i, v_i, {w_b}_i$ and ${w_s}_i$ are the unknowns to be found, ω is the natural frequency of the bi-directional FGP, $i = \sqrt{-1}$ is the complex number, $\psi_i(x,y), \lambda_i(x,y), \Delta_i(x,y)$ and $\Omega_i(x,y)$ are the shape functions, $p_\Theta, q_\Theta, r_\Theta, s_\Theta$ $(\Theta = \mathrm{u, v}, w_b, w_s)$ are the boundary exponents which controls the various boundary conditions [69]. The boundary exponents takes the values 0, 1 or 2 accordingly as the side x=0, a; y=0, b; is free, simply supported or clamped respectively.

The fifteen components of admissible functions of ϕ_i (i=1, 2, 3……15) are obtained from Pascal's triangle and is given below.

$$\phi_1 = 1;\ \phi_2 = x; \phi_3 = y; \phi_4 = x^2; \phi_5 = xy; \phi_6 = y^2; \phi_7 = x^3;$$
$$\phi_8 = x^2y; \phi_9 = xy^2; \phi_{10} = y^3; \phi_{11} = x^4; \phi_{12} = x^3y;$$
$$\phi_{13} = x^2y^2; \phi_{14} = xy^3; \phi_{15} = y^4 \quad (12)$$

Substitution of Eqs. (11) into Eqs. (8) and (10), the equations of motion can be obtained and then using the Lagrange equations

$$\frac{\partial U}{\partial C_j} + \frac{\partial}{\partial t}\left(\frac{\partial K}{\partial \dot{C}_j}\right) = 0 \quad (13)$$

Where C_j denoting the values of $(u_i, v_i, {w_b}_i$ and ${w_s}_i)$ that leads to

$$\begin{bmatrix} [S_{11}] & [S_{12}] & [S_{13}] & [S_{14}] \\ [S_{12}]^T & [S_{22}] & [S_{23}] & [S_{24}] \\ [S_{13}]^T & [S_{23}]^T & [S_{33}] & [S_{34}] \\ [S_{14}]^T & [S_{24}]^T & [S_{34}]^T & [S_{44}] \end{bmatrix} - \omega^2 \begin{bmatrix} [M_{11}] & [M_{12}] & [M_{13}] & [M_{14}] \\ [M_{12}]^T & [M_{22}] & [M_{23}] & [M_{24}] \\ [M_{13}]^T & [M_{23}]^T & [M_{33}] & [M_{34}] \\ [M_{14}]^T & [M_{24}]^T & [M_{34}]^T & [M_{44}] \end{bmatrix} \begin{Bmatrix} \{u\} \\ \{v\} \\ \{w_b\} \\ \{w_s\} \end{Bmatrix} = \begin{Bmatrix} \{0\} \\ \{0\} \\ \{0\} \\ \{0\} \end{Bmatrix} \quad (14)$$

Where $[S_{mn}]$ are the stiffness matrices and and $[M_{mn}]$ are the mass matrices. The components of $[S_{mn}]$ and $[M_{mn}]$ are given as

$$S_{11}(i,j) = \int_0^a\int_0^b\int_{-h/2}^{h/2}\left(\frac{E(x,z)}{1-\mu^2}\psi_{i,x}\psi_{j,x} + \frac{E(x,z)}{2(1+\mu)}\psi_{i,y}\psi_{j,y}\right)dzdydx$$

$$S_{12}(i,j) = \int_0^a\int_0^b\int_{-h/2}^{h/2}\left(\frac{\mu E(x,z)}{1-\mu^2}\psi_{i,x}\lambda_{j,y} + \frac{E(x,z)}{2(1+\mu)}\psi_{i,y}\lambda_{j,x}\right)dzdydx$$

$$S_{13}(i,j) = -\int_0^a\int_0^b\int_{-h/2}^{h/2} z\left(\frac{E(x,z)}{1-\mu^2}\psi_{i,x}\Delta_{j,xx} + \frac{\mu E(x,z)}{1-\mu^2}\psi_{i,x}\Delta_{j,yy} + \frac{E(x,z)}{(1+\mu)}\psi_{i,y}\Delta_{j,xy}\right)dzdydx$$

$$S_{14}(i,j) = 0$$

$$S_{22}(i,j) = \int_0^a\int_0^b\int_{-h/2}^{h/2}\left(\frac{E(x,z)}{1-\mu^2}\lambda_{i,y}\lambda_{j,y} + \frac{E(x,z)}{2(1+\mu)}\lambda_{i,x}\lambda_{j,x}\right)dzdydx$$

$$S_{23}(i,j) = -\int_0^a\int_0^b\int_{-h/2}^{h/2} z\left(\frac{E(x,z)}{1-\mu^2}\lambda_{i,y}\Delta_{j,yy} + \frac{\mu E(x,z)}{1-\mu^2}\lambda_{i,y}\Delta_{j,xx} + \frac{E(x,z)}{(1+\mu)}\lambda_{i,x}\Delta_{j,xy}\right)dzdydx$$

$$S_{24}(i,j) = 0$$

$$S_{33}(i,j) = \int_0^a\int_0^b\int_{-h/2}^{h/2} z^2\left(\frac{E(x,z)}{1-\mu^2}\left(\Delta_{i,xx}\Delta_{j,xx} + \Delta_{i,yy}\Delta_{j,yy}\right) + 2\frac{\mu E(x,z)}{1-\mu^2}\Delta_{i,xx}\Delta_{j,yy} + 2\frac{E(x,z)}{(1+\mu)}\Delta_{i,xy}\Delta_{j,xy}\right)dzdydx$$

$$S_{34}(i,j) = 0$$

$$S_{44}(i,j) = \int_0^a\int_0^b\int_{-h/2}^{h/2}\left(1-\left(\frac{2z}{h}\right)^{p-1}\right)^2\frac{E(x,z)}{2(1+\mu)}\left(\Omega_{i,x}\Omega_{j,x} + \Omega_{i,y}\Omega_{j,y}\right)dzdydx$$

$$M_{11}(i,j) = \int_0^a\int_0^b\int_{-h/2}^{h/2}\rho\psi_i\psi_j dzdydx$$

$$M_{12}(i,j) = 0$$

$$M_{13}(i,j) = -\int_0^a\int_0^b\int_{-h/2}^{h/2}\rho\psi_i\Delta_{j,x}dzdydx$$

$$M_{14}(i,j) = 0$$

$$M_{22}(i,j) = \int_0^a\int_0^b\int_{-h/2}^{h/2}\rho\lambda_i\lambda_j dzdydx$$

$$M_{23}(i,j) = -\int_0^a\int_0^b\int_{-h/2}^{h/2}\rho z\lambda_i\Delta_{j,y}dzdydx$$

$$M_{24}(i,j) = 0$$

$$M_{33}(i,j) = \int_0^a\int_0^b\int_{-h/2}^{h/2}\rho\left(z^2\left(\Delta_{i,x}\Delta_{j,x} + \Delta_{i,y}\Delta_{j,y}\right) + \Delta_i\Delta_j\right)dzdydx$$

$$M_{34}(i,j) = \int_0^a\int_0^b\int_{-h/2}^{h/2}\rho z^2\Delta_i\Omega_j dzdydx$$

$$M_{44}(i,j) = \int_0^a\int_0^b\int_{-h/2}^{h/2}\rho z^2\Omega_i\Omega_j dzdydx,\ \mathrm{i, j}=1, 2\ldots\ldots$$

3. Results and Discussion

This section discusses the influence of thickness ratio, aspect ratio, gradation indexes, type of porosity and volume fraction of porosity on the free vibration analysis of bi-directional FGPs.

The numerical investigations are carried out for simply supported boundary conditions and are set as.

v=w_b=w_s=0 @ x=0, a; u= w_b=w_s=0 @ y=0, b

The material properties are given in Table 1. The following dimensionless frequency parameters are used for the representation of results.

$$\widehat{\omega} = \omega h \sqrt{\frac{\rho_m}{E_m}};\ \bar{\omega} = \omega \frac{a^2}{h} \sqrt{\frac{\rho_c}{E_c}}$$

To validate the RFSDT, convergence studies are performed by varying the number of components (k) of ϕ_i and the order of shear strains shape function. The numerical results are presented in non-dimensional form in Tables 3-4 and compared with (i) 3-D exact solutions provided by Vel and Batra [70] (ii) Hosseini-Hashemi et al. [71], Sidda Reddy et al.[16] and Nguyen Van Long et al. [72] based on third order shear deformation theory of perfect FGP.

The material properties presented in Table 2 are used to compute the results of Table 3 and 4.

Table 2: Material properties of perfect FGP

Properties of the material	Al	Al_2O_3	ZrO_2
E (GPa)	70	380	200
$\rho\ (kg/m^3)$	2702	3800	5700
μ	0.3	0.3	0.3

From Tables 3 and 4, it is observed that the RFSDT results with Order p=9 and the number of components in ϕ_i 12 and 15 are well agreeing with HSDTs [16, 71-72] and 3-D exact solutions [70]. Hence, the RFSDT results should provide the benchmark results for future comparisons.

From Table 4, it is noticed that, the absolute difference $(\frac{\text{Present}-\text{3D}}{\text{Present}} \times 100)$ decreases with increase of side-to-thickness ratio, and power law exponent (n). From an accuracy point of view, 15 components of ϕ_i are considered in analyzing the extensive free vibration of simply supported porous bidirectional FGPs.

Table 3: Dimensionless fundamental frequency $\bar{\omega}$ for all sides simply supported Al/Al_2O_3 perfect square FG plate.

a/h	Order	Method	Power-law index (n)				
	)		0	0.5	1	4	10
5		TSDT[71]	0.2113	0.1807	0.1631	0.1378	0.1301
		TSDT[72]	0.228	0.1949	0.1765	0.1504	0.142
	Present (with No. of terms, k)						
	7	k=10	0.2103	0.1801	0.1625	0.1377	0.1295
		k=12	0.2103	0.1801	0.1625	0.1377	0.1295
	9	K=10	0.2113	0.1808	0.1632	0.1386	0.1306
		K=12	0.2113	0.1808	0.1632	0.1386	0.1306
		K=15	0.2113	0.1808	0.1632	0.1386	0.1306
10		TSDT[71]	0.0577	0.049	0.0442	0.0381	0.0364
		TSDT[72]	0.0591	0.0502	0.0457	0.0402	0.0383
		Present (with No. of terms, k)					
	7	k=6	0.0576	0.0492	0.0446	0.0386	0.0366
		k=8	0.0576	0.0491	0.0443	0.0383	0.0365
		k=10	0.0576	0.0490	0.0442	0.0381	0.0363
		k=12	0.0576	0.0490	0.0442	0.0381	0.0363
	9	k=15	0.0577	0.0490	0.0442	0.0381	0.0364
20		TSDT[71]	0.0148	0.0125	0.0113	0.0098	0.0094
		TSDT[72]	0.0154	0.013	0.0119	0.0105	0.01
	9	k=15	0.0148	0.0126	0.0113	0.0098	0.0094

Table 4: Fundamental frequency $\widehat{\omega}$ for all sides simply supported Al/ZrO_2 perfect square FG plate.

Method	n =1			a/h= 5		
	a/h=20	a/h=10	a/h=5	n =2	n =3	n =5
HSDT[16]	-	0.0619	0.2285	0.2264	0.2271	0.2281
HSDT[71]	0.0158	0.0619	0.2276	0.2256	0.2263	0.2272
3-D [70]	0.0153	0.0596	0.2192	0.2197	0.2211	0.2225
Present k=15	0.0158	0.0619	0.2277	0.2260	0.2268	0.2279
|Diff(%) |	3.41%	3.67%	3.74%	2.77%	2.53%	2.37%

In Tables 5-8, the first ten nondimensionalized natural frequencies of the bidirectional FGPs with all sides simply supported conditions are presented using the present RFSDT for two different side-to-thickness ratios, (a/h=2 and 5), several gradation index values in both directions (x-direction, η_1=0, 1, 2 & 10 and z-direction, η_2=0, 1, 2 & 10), various values of porosity volume fraction (γ=0, 0.1 & 0.2) and two types of distributions of porosities (even porosity and uneven porosity).

The bi-directional FGPs natural frequency in Tables 5-8 is a function of several parameters; therefore, its behavior is usually more complicated than those of one directional FGPs. The complicated properties of the bidirectional FGPs can generate the complexity of the natural frequency here.

In the results of natural frequencies shown in Table 5-6, we can see the strong influence of the gradation indexes, side to thickness ratios, type of porosity and volume fraction of porosity on the dimensionless frequency. The higher the gradation indexes are, the lower the obtained natural frequencies are. This is the result of a decrease of the contribution of the stronger ceramic phase with the increase of gradation indexes. This causes the decreasing the stiffness as well as the raising the mass density of the bidirectional FGP. From the vibration theory, it is very well known that the vibration frequency is inversely propositional to the mass, whilst it is directly proportional to the stiffness of the plate, e.g. modulus of elasticity. Also, we can see that the dependence of the natural frequency of bidirectional FGPs on the gradation indexes η_1 and η_2, volume fraction of porosity and type of porosity is clear, which may be noting through the effective Young's modulus (see Figure 3).

From the tables it is realized that, the higher the side to thickness ratio is, the higher the dimensionless natural frequency $\bar{\omega}$ is, for both even and uneven porosity distributions whilst, it decreases with the increase of gradation indexes. This shows that the thinner the bidirectional FGP is, the lower the natural frequency ω is. This is due to the less rigidity to thin plates. Also note that the natural frequency ω is expressed in dimensionless formula $\bar{\omega}$ is inversely proportional to the plate thickness (h).

In Tables 5-6, it is noticed that, in even porosity distribution the natural frequency increases for the gradation index values η_2=0 & 1 and then it decreases for both a/h=2 & 5, while it increases with increase of η_2 in case of uneven porosity distribution. Again, it is observed that, natural frequencies unaltered for both even and uneven porosity distributions when η_2=0 and at all the values of η_1.

Figure 4 and 5 depict the influence of volume fraction of porosity and gradation indexes on the dimensionless natural frequency of a bidirectional square FGP for even and uneven porosity distributions respectively, at a/h=10. The vibration behavior of even porosity distribution is entirely different from the uneven porosity distribution. Moreover, for even porosity distribution, at lower values of gradation index η_2 values, the dimensionless natural frequency increases with the increase of volume fraction of porosity, while it decreases at higher values of gradation index, η_2 values. Again the reason is, the mass of the plate is a bit more dominant than the modulus of elasticity. The gradation indexes have no influence on the dimensionless fundamental frequency at some specific values, for example, at η_1=0, η_2=10; and η_1=1, η_2=5; for a specific value of the porosity volume fraction, γ=0.2435. In the case of uneven porosity distributions, the fundamental frequencies increase with the increase of volume fraction of porosity and gradation indexes (see Figure 5). The increase of volume fraction of porosity decreases the mass of the plate and increases the stiffness. Furthermore, higher the gradation indexes, the lower the obtained dimensionless fundamental frequencies. In this case also, the gradation indexes have no influence on dimensionless fundamental frequency at η_1=0, η_2=10; and η_1=10, η_2=1; for a specific value of the porosity volume fraction, γ=0.2615.

The influence of aspect ratio, gradation indexes and volume fraction of porosity on the fundamental frequency are shown in Figures 6 and 7 for even and uneven porosity distributions respectively, at a/h=10. For completely homogenous plates i.e., η_1=0, η_2=0, the fundamental frequencies increase with the increase of volume fraction of porosity, while they decrease with the increase of volume fraction of porosity in bidirectional FGPs for even porosity distributions (see Figure 6). The reason is that for completely homogeneous plates, modulus of elasticity is a bit more dominant than the mass of the plate. In the case of uneven porosity distributions, the higher the volume fraction of porosities is, the higher the fundamental frequency is, for both completely homogeneous and bidirectional FGPs. Furthermore, the increment of aspect ratio b/a, decrease the fundamental frequencies for both even and uneven porosity distributions. Also, observed that the fundamental frequencies are higher for uneven porosity distributions compared to even porosity distributions. Again, it is clear that, the effective modulus of elasticity is higher for uneven porosity distributions comparing to even porosity distributions (see Figure 3).

4. Conclusions

In the present paper, a refined first order shear deformation is developed to investigate the free vibration behavior of bidirectional FGPs. The present theory satisfies the nullity conditions at the top and bottom of the plate for the transverse shear stresses. This avoids the need of a shear correction factor. The material properties of the bidirectional porous FGPs are changed by employing the gradation indexes in both x-direction and z-direction and volume fraction of porosity. The equilibrium equations of motion are obtained through Lagrange equations in combination with polynomials and added admissible functions which are used to fulfill the boundary conditions. The admissible functions are generated using Pascal's triangle. Several gradation indexes values for both x-direction and z-direction, side-to-thickness ratios, aspect ratios, type of porosity and volume fraction of porosity are considered. The computed natural frequencies are represented in dimensionless form and compared with the results of previous studies. It is established that the computed results of the present refined first order shear deformation theory match very well with the result available in the literature. To understand the vibration behavior of bidirectional FGPs, exhaustive analysis is performed by varying the gradation indexes, side-to- thickness ratios, aspect ratios, type of porosity and volume fraction of porosity.

It is concluded that the nondimensionalized natural frequencies increase with increase of side to thickness ratio, while they decrease as the aspect ratio and gradation indexes in x and z directions increase for both types of porosity distributions. For lower values of gradation indexes, the natural frequencies increase with increase of porosity, while they decrease at higher values of gradation indexes. The presented numerical results can be used as benchmark solutions to assess the various plate theories and compare with solutions obtained by other analytical and finite element methods. From the present work, it can be concluded that the present theory allows examining the vibration behavior of bidirectional porous FG plates manufactured in the sintering process.

Table 5: Influence of volume fraction exponents, porosity volume fraction on First ten dimensionless natural frequencies of a simply supported bidirectional FG porous square plate, a/h=2 (Even porosity distribution)

η_1	η_2	γ	$\bar{\omega}_1$	$\bar{\omega}_2$	$\bar{\omega}_3$	$\bar{\omega}_4$	$\bar{\omega}_5$	$\bar{\omega}_6$	$\bar{\omega}_7$	$\bar{\omega}_8$	$\bar{\omega}_9$	$\bar{\omega}_{10}$
0	0	0	5.1707	5.4314	5.4314	7.6853	9.5276	9.5276	10.8661	10.8661	12.1784	12.1784
		0.1	5.4442	5.7188	5.7188	8.0920	10.0317	10.0317	11.4410	11.4410	12.8228	12.8228
		0.2	5.9097	6.2078	6.2078	8.7838	10.8895	10.8895	12.4192	12.4192	13.9191	13.9191
	1	0	4.4777	4.7662	4.7662	6.7439	8.2870	8.2870	9.5351	9.5351	10.6867	10.6867
		0.1	4.5715	4.9023	4.9023	6.9365	8.4808	8.4808	9.8075	9.8075	10.992	10.992
		0.2	4.7255	5.1513	5.1513	7.2886	8.811	8.811	10.3056	10.3056	11.5503	11.5503
	2	0	4.2561	4.505	4.505	6.3742	7.8323	7.8323	9.0125	9.0125	10.101	10.101
		0.1	4.2809	4.5686	4.5686	6.4642	7.8908	7.8908	9.1398	9.1398	10.2437	10.2437
		0.2	4.2961	4.6891	4.6891	6.6345	7.9604	7.9604	9.3809	9.3809	10.5139	10.5139
	10	0	3.9135	4.0761	4.0761	5.7675	7.1245	7.1245	8.1546	8.1546	9.1395	9.1395
		0.1	3.8396	4.0002	4.0002	5.66	6.9653	6.9653	8.0027	8.0027	8.9692	8.9692
		0.2	3.6686	3.8453	3.8453	5.4408	6.6147	6.6147	7.6928	7.6928	8.6219	8.6219
1	0	0	5.1706	5.4314	5.4314	7.6853	9.5276	9.5276	10.8661	10.8661	12.1784	12.1784
		0.1	5.4442	5.7188	5.7188	8.092	10.0317	10.0317	11.441	11.441	12.8228	12.8228
		0.2	5.9097	6.2078	6.2078	8.7838	10.8894	10.8894	12.4192	12.4192	13.9191	13.9191
	1	0	4.293	4.4922	4.5175	6.5027	7.9278	7.9452	8.9777	9.0716	10.1803	10.3193
		0.1	4.3276	4.5216	4.5578	6.607	7.9988	8.0252	9.0311	9.1677	10.2925	10.4939
		0.2	4.376	4.561	4.6166	6.7756	8.1014	8.1457	9.1005	9.3146	10.4612	10.7756
	2	0	4.0805	4.2507	4.2811	6.2227	7.5381	7.5529	8.5183	8.613	9.6661	9.8404
		0.1	4.0716	4.2347	4.2739	6.2759	7.5341	7.5544	8.4922	8.618	9.6722	9.9116
		0.2	4.0527	4.2105	4.261	6.3663	7.5258	7.5546	8.4523	8.6266	9.6746	10.012
	10	0	3.8113	3.9345	3.971	5.8685	7.0334	7.0342	7.9509	8.0118	8.9934	9.2034
		0.1	3.7575	3.8643	3.9051	5.863	6.9372	6.9448	7.8435	7.9036	8.8715	9.1458
		0.2	3.6728	3.7639	3.8014	5.8654	6.7858	6.8121	7.6953	7.7368	8.6784	9.0361
2	0	0	5.1706	5.4314	5.4314	7.6853	9.5276	9.5276	10.8661	10.8661	12.1784	12.1784
		0.1	5.4442	5.7188	5.7188	8.092	10.0317	10.0317	11.441	11.441	12.8228	12.8228
		0.2	5.9097	6.2078	6.2078	8.7838	10.8894	10.8894	12.4192	12.4192	13.9191	13.9191
	1	0	4.2008	4.3526	4.4435	6.4766	7.7858	7.8221	8.893	8.9032	10.0377	10.2782
		0.1	4.2167	4.3595	4.4622	6.5592	7.8254	7.8718	8.9317	8.9575	10.1086	10.4135
		0.2	4.2376	4.3681	4.4858	6.6831	7.8802	7.9432	8.9816	9.0361	10.2062	10.5755
	2	0	3.9894	4.1068	4.2156	6.2193	7.4144	7.442	8.4555	8.4617	9.546	9.8324
		0.1	3.9699	4.0723	4.1955	6.2578	7.3933	7.4248	8.4318	8.4335	9.5276	9.8678
		0.2	3.9403	4.0219	4.1655	6.3168	7.3633	7.3988	8.3934	8.3974	9.4948	9.8638
	10	0	3.7363	3.8005	3.9324	5.9114	6.9613	6.9645	7.8982	7.9491	8.9367	9.2753
		0.1	3.6826	3.7191	3.8708	5.9057	6.8721	6.8786	7.7869	7.8571	8.822	9.1805
		0.2	3.5994	3.6066	3.7835	5.903	6.7357	6.7645	7.6243	7.7347	8.6517	9.0208
10	0	0	5.1706	5.4314	5.4314	7.6853	9.5276	9.5276	10.8661	10.8661	12.1784	12.1784
		0.1	5.4442	5.7188	5.7188	8.092	10.0317	10.0317	11.441	11.441	12.8228	12.8228
		0.2	5.9097	6.2078	6.2078	8.7838	10.8894	10.8894	12.4192	12.4192	13.9191	13.9191
	1	0	4.1348	4.2551	4.4001	6.3387	7.6419	7.6673	8.6506	8.8142	9.8005	10.0514
		0.1	4.1394	4.2445	4.4127	6.3773	7.6541	7.6844	8.6543	8.8436	9.8125	10.1143
		0.2	4.1448	4.2281	4.4286	6.4297	7.6693	7.7069	8.6574	8.8823	9.8226	10.1994
	2	0	3.9339	4.0211	4.196	6.0816	7.2782	7.3237	8.2155	8.417	9.3345	9.6291
		0.1	3.9112	3.9777	4.1789	6.0826	7.239	7.2944	8.1584	8.3909	9.2815	9.627
		0.2	3.8807	3.9171	4.1551	6.0842	7.1851	7.2557	8.0802	8.3562	9.207	9.6209
	10	0	3.7099	3.7444	3.9595	5.7906	6.8565	6.9323	7.7091	7.9644	8.8006	9.1436
		0.1	3.6642	3.668	3.9154	5.7593	6.7695	6.8632	7.5948	7.8907	8.6903	9.0835
		0.2	3.5627	3.6047	3.8571	5.7205	6.6537	6.7753	7.4425	7.7974	8.5447	8.9666

Table 6: Influence of volume fraction exponents, porosity volume fraction on First ten dimensionless natural frequencies of a simply supported bidirectional FG porous square plate, a/h=5 (Even porosity distribution)

η_1	η_2	γ	$\bar{\omega}_1$	$\bar{\omega}_2$	$\bar{\omega}_3$	$\bar{\omega}_4$	$\bar{\omega}_5$	$\bar{\omega}_6$	$\bar{\omega}_7$	$\bar{\omega}_8$	$\bar{\omega}_9$	$\bar{\omega}_{10}$
0	0	0	7.3623	13.5786	13.5786	16.1407	16.1407	19.2133	23.3645	27.1651	27.1651	27.7458
		0.1	7.7519	14.2971	14.2971	16.9947	16.9947	20.2299	24.6008	28.6025	28.6025	29.2139
		0.2	8.4147	15.5195	15.5195	18.4477	18.4477	21.9596	26.7042	31.0480	31.0480	31.7117
	1	0	6.3336	11.9154	11.9154	13.9243	13.9243	16.8596	20.2868	23.8378	23.8378	24.1684
		0.1	6.4431	12.2558	12.2558	14.1866	14.1866	17.3411	20.7419	24.5188	24.5188	24.7550
		0.2	6.6096	12.8782	12.8782	14.6004	14.6004	18.2214	21.5082	25.7640	25.7640	25.7726
	2	0	6.0838	11.2624	11.2624	13.3119	13.3119	15.9356	19.3557	22.5314	22.5314	23.0321
		0.1	6.1070	11.4215	11.4215	13.3730	13.3730	16.1604	19.5235	22.8496	22.8496	23.2791
		0.2	6.0858	11.7227	11.7227	13.3647	13.3647	16.5861	19.7155	23.4523	23.4523	23.6419
	10	0	5.7008	10.1903	10.1903	12.3696	12.3696	14.4188	17.8205	20.3865	20.3865	21.1061
		0.1	5.6340	10.0004	10.0004	12.1836	12.1836	14.1501	17.5401	20.0067	20.0067	20.7636
		0.2	5.4561	9.6132	9.6132	11.7236	11.7236	13.6019	16.8816	19.2320	19.2320	19.9802
1	0	0	7.3623	13.5786	13.5786	16.1407	16.1407	19.2133	23.3645	27.1651	27.1651	27.7458
		0.1	7.7519	14.2971	14.2971	16.9947	16.9947	20.2299	24.6008	28.6025	28.6025	29.2139
		0.2	8.4147	15.5195	15.5195	18.4477	18.4477	21.9596	26.7042	31.0480	31.0480	31.7117
	1	0	6.1112	11.2220	11.2937	13.4216	13.4476	16.2577	19.4737	22.4437	22.6789	23.0953
		0.1	6.1598	11.2916	11.3944	13.5384	13.5774	16.5187	19.6640	22.5770	22.9192	23.3047
		0.2	6.2279	11.3828	11.5414	13.7060	13.7706	16.9402	19.9472	22.7500	23.2865	23.6082
	2	0	5.8180	10.6122	10.7028	12.7822	12.8137	15.5580	18.5516	21.2950	21.5325	21.9918
		0.1	5.8090	10.5633	10.6849	12.7753	12.8171	15.6916	18.5588	21.2294	21.5451	21.9913
		0.2	5.7900	10.4824	10.6526	12.7587	12.8153	15.9183	18.5609	21.1286	21.5665	21.9862
	10	0	5.4413	9.8302	9.9275	11.9529	11.9803	14.6717	17.3459	19.8772	20.0295	20.5595
		0.1	5.3714	9.649	9.7627	11.8105	11.8379	14.6581	17.1459	19.6086	19.759	20.327
		0.2	5.2674	9.3812	9.5036	11.6023	11.619	14.6646	16.8431	19.2379	19.3421	19.9958
2	0	0	7.3623	13.5786	13.5786	16.1407	16.1407	19.2133	23.3645	27.1651	27.1651	27.7458
		0.1	7.7519	14.2971	14.2971	16.9947	16.9947	20.2299	24.6008	28.6025	28.6025	29.2139
		0.2	8.4147	15.5195	15.5195	18.4477	18.4477	21.9596	26.7042	31.048	31.048	31.7117
	1	0	5.9827	10.8814	11.1023	13.1802	13.2563	16.1922	19.194	22.2326	22.2579	22.7199
		0.1	6.0052	10.8987	11.1466	13.2444	13.3398	16.3988	19.316	22.3294	22.3938	22.8433
		0.2	6.0347	10.9201	11.2014	13.3325	13.4586	16.7089	19.4899	22.4541	22.5902	23.0142
	2	0	5.6769	10.267	10.5301	12.5353	12.6143	15.5489	18.2754	21.1387	21.1546	21.6423
		0.1	5.6495	10.1809	10.4759	12.4947	12.5865	15.6453	18.2393	21.0794	21.0842	21.5922
		0.2	5.6092	10.0546	10.3929	12.4363	12.544	15.7934	18.185	20.9843	20.9936	21.5228
	10	0	5.3184	9.5013	9.8284	11.7682	11.8302	14.7786	17.1537	19.7455	19.873	20.3513
		0.1	5.2446	9.2977	9.6727	11.6271	11.6873	14.7645	16.9565	19.4674	19.643	20.134
		0.2	5.1432	8.9984	9.4512	11.4356	11.4831	14.7578	16.679	19.0608	19.3375	19.8311
10	0	0	7.3623	13.5786	13.5786	16.1407	16.1407	19.2133	23.3645	27.1651	27.1651	27.7458
		0.1	7.7519	14.2971	14.2971	16.9947	16.9947	20.2299	24.6008	28.6025	28.6025	29.2139
		0.2	8.4147	15.5195	15.5195	18.4477	18.4477	21.9596	26.7042	31.048	31.048	31.7117
	1	0	5.8872	10.6376	10.9989	12.9735	12.983	15.8476	18.8066	21.6266	22.0364	22.3872
		0.1	5.8932	10.6112	11.0301	12.9987	13.0091	15.9447	18.8496	21.6358	22.1101	22.4468
		0.2	5.9002	10.5702	11.0692	13.0309	13.0422	16.076	18.9062	21.6434	22.2071	22.5258
	2	0	5.5818	10.0527	10.4885	12.3382	12.3413	15.2048	17.9018	20.5389	21.0434	21.3156
		0.1	5.5477	9.9443	10.4453	12.2754	12.2822	15.2074	17.8207	20.3961	20.9784	21.2226
		0.2	5.5023	9.7927	10.3848	12.1906	12.2042	15.2116	17.7132	20.2004	20.8921	21.0964
	10	0	5.2653	9.3611	9.8983	11.6396	11.6672	14.4766	16.9006	19.2727	19.9113	20.1024
		0.1	5.2016	9.17	9.7879	11.5042	11.5432	14.3984	16.7163	18.9871	19.727	19.8739
		0.2	5.1207	8.9067	9.6421	11.3289	11.3868	14.3013	16.4814	18.6063	19.4938	19.5739

Table 7: Influence of volume fraction exponents, porosity volume fraction on First ten dimensionless natural frequencies of a simply supported bidirectional FG porous square plate, a/h=2 (Uneven porosity distribution)

η_1	η_2	γ	$\bar{\omega}_1$	$\bar{\omega}_2$	$\bar{\omega}_3$	$\bar{\omega}_4$	$\bar{\omega}_5$	$\bar{\omega}_6$	$\bar{\omega}_7$	$\bar{\omega}_8$	$\bar{\omega}_9$	$\bar{\omega}_{10}$
0	0	0.1	5.3126	5.5587	5.5587	7.8654	9.7486	9.7486	11.1207	11.1207	12.4638	12.4638
		0.2	5.4857	5.7188	5.7188	8.0920	10.0204	10.0204	11.4410	11.4410	12.8228	12.8228
	1	0.1	4.5533	4.8256	4.8256	6.8279	8.3833	8.3833	9.6540	9.6540	10.8199	10.8199
		0.2	4.6437	4.9023	4.9023	6.9365	8.4987	8.4987	9.8075	9.8075	10.9920	10.9920
	2	0.1	4.3007	4.5325	4.5325	6.4132	7.8645	7.8645	9.0677	9.0677	10.1628	10.1628
		0.2	4.3491	4.5686	4.5686	6.4642	7.8944	7.8944	9.1398	9.1398	10.2437	10.2437
	10	0.1	3.9077	4.0437	4.0437	5.7216	7.0448	7.0448	8.0897	8.0897	9.0668	9.0668
		0.2	3.8822	4.0002	4.0002	5.6601	6.9134	6.9134	8.0027	8.0027	8.9692	8.9692
1	0	0.1	5.3126	5.5587	5.5587	7.8654	9.7486	9.7486	11.1207	11.1207	12.4638	12.4638
		0.2	5.4857	5.7188	5.7188	8.0920	10.0204	10.0204	11.4410	11.4410	12.8228	12.8228
	1	0.1	4.3308	4.5062	4.5359	6.5493	7.9648	7.9858	9.0027	9.1151	10.2311	10.3972
		0.2	4.3719	4.5225	4.5578	6.6070	8.0043	8.0300	9.0310	9.1677	10.2922	10.4939
	2	0.1	4.0974	4.2442	4.2780	6.2461	7.5404	7.5567	8.5065	8.6152	9.6690	9.8723
		0.2	4.1126	4.2369	4.2739	6.2759	7.5383	7.5558	8.4920	8.6180	9.6717	9.9110
	10	0.1	3.8065	3.9028	3.9412	5.8651	6.9902	6.9962	7.9012	7.9627	8.9384	9.1772
		0.2	3.7952	3.8662	3.9051	5.8630	6.9303	6.9455	7.8435	7.9036	8.8715	9.1443
2	0	0.1	5.3126	5.5587	5.5587	7.8654	9.7486	9.7486	11.1207	11.1207	12.4638	12.4638
		0.2	5.4857	5.7188	5.7188	8.0920	10.0204	10.0204	11.4410	11.4410	12.8228	12.8228
	1	0.1	4.2275	4.3558	4.4524	6.5141	7.8081	7.8481	8.9112	8.9281	10.0703	10.3398
		0.2	4.2558	4.3595	4.4625	6.5592	7.8304	7.8747	8.9316	8.9575	10.1082	10.4107
	2	0.1	3.9990	4.0910	4.2067	6.2366	7.4090	7.4369	8.4446	8.4487	9.5378	9.8502
		0.2	4.0069	4.0723	4.1960	6.2578	7.3993	7.4265	8.4318	8.4334	9.5272	9.8530
	10	0.1	3.7287	3.7632	3.9041	5.9083	6.9234	6.9272	7.8471	7.9061	8.8843	9.2275
		0.2	3.7167	3.7191	3.8709	5.9057	6.8694	6.8842	7.7869	7.8571	8.8220	9.1500
10	0	0.1	5.3126	5.5587	5.5587	7.8654	9.7486	9.7486	11.1207	11.1207	12.4638	12.4638
		0.2	5.4857	5.7188	5.7188	8.0920	10.0204	10.0204	11.4410	11.4410	12.8228	12.8228
	1	0.1	4.1539	4.2503	4.4061	6.3566	7.6493	7.6789	8.6525	8.8280	9.8064	10.0806
		0.2	4.1734	4.2445	4.4127	6.3773	7.6543	7.6891	8.6543	8.8436	9.8121	10.1143
	2	0.1	3.9396	4.001	4.1881	6.0821	7.2621	7.3147	8.189	8.4048	9.31	9.6282
		0.2	3.9439	3.9777	4.179	6.0827	7.2403	7.3019	8.1584	8.3909	9.2813	9.6268
	10	0.1	3.703	3.709	3.9388	5.7758	6.8173	6.9048	7.6557	7.9296	8.749	9.1155
		0.2	3.668	3.6933	3.9154	5.7593	6.7696	6.8718	7.5948	7.8907	8.6903	9.0744

Table 8: Influence of volume fraction exponents, porosity volume fraction on First ten dimensionless natural frequencies of a simply supported bidirectional FG porous square plate, a/h=5 (Uneven porosity distribution)

η_1	η_2	γ	$\bar{\omega}_1$	$\bar{\omega}_2$	$\bar{\omega}_3$	$\bar{\omega}_4$	$\bar{\omega}_5$	$\bar{\omega}_6$	$\bar{\omega}_7$	$\bar{\omega}_8$	$\bar{\omega}_9$	$\bar{\omega}_{10}$
0	0	0.1	7.6343	13.8968	13.8968	16.6641	16.6641	19.6636	24.0611	27.8018	27.8018	28.5368
		0.2	7.9668	14.2971	14.2971	17.3019	17.3019	20.2299	24.9099	28.6025	28.6025	29.5013
	1	0.1	6.5132	12.0639	12.0639	14.2438	14.2438	17.0697	20.7015	24.1349	24.1349	24.6307
		0.2	6.7319	12.2558	12.2558	14.6286	14.6286	17.3412	21.1998	24.5188	24.5188	25.1859
	2	0.1	6.2317	11.3313	11.3313	13.5483	13.5483	16.033	19.6425	22.6692	22.6692	23.3375
		0.2	6.4076	11.4215	11.4215	13.8202	13.8202	16.1605	19.9674	22.8496	22.8496	23.6801
	10	0.1	5.8126	10.1092	10.1092	12.4886	12.4886	14.3041	17.8936	20.2243	20.2243	21.1325
		0.2	5.9369	10.0004	10.0004	12.5872	12.5872	14.1501	17.9052	20.0067	20.0067	21.0679
1	0	0.1	7.6343	13.8968	13.8968	16.6641	16.6641	19.6636	24.0611	27.8018	27.8018	28.5368
		0.2	7.9668	14.2971	14.2971	17.3019	17.3019	20.2299	24.9099	28.6025	28.6025	29.5013
	1	0.1	6.2233	11.2546	11.3398	13.6114	13.6453	16.3743	19.7091	22.5062	22.7878	23.3321
		0.2	6.3515	11.2916	11.3944	13.825	13.8698	16.5187	19.9742	22.577	22.9192	23.5943
	2	0.1	5.9008	10.5905	10.695	12.911	12.9494	15.6168	18.6984	21.2654	21.538	22.1273
		0.2	5.9933	10.5633	10.6849	13.0509	13.0979	15.6916	18.8552	21.2293	21.5451	22.2682
	10	0.1	5.4924	9.7475	9.8531	12.014	12.0431	14.6634	17.3891	19.7527	19.9068	20.5819
		0.2	5.5472	9.649	9.7627	12.0736	12.1018	14.6581	17.419	19.6085	19.759	20.5889
2	0	0.1	7.6343	13.8968	13.8968	16.6641	16.6641	19.6636	24.0611	27.8018	27.8018	28.5368
		0.2	7.9668	14.2971	14.2971	17.3019	17.3019	20.2299	24.9099	28.6025	28.6025	29.5013
	1	0.1	6.0733	10.8896	11.1233	13.3321	13.4196	16.286	19.3848	22.2781	22.3202	22.9037
		0.2	6.1748	10.8987	11.1467	13.4997	13.6012	16.3988	19.5951	22.3294	22.3938	23.1029
	2	0.1	5.7403	10.2276	10.5057	12.6334	12.7208	15.5924	18.388	21.1115	21.1222	21.7414
		0.2	5.8097	10.1809	10.476	12.7382	12.8348	15.6454	18.5056	21.0794	21.0841	21.8424
	10	0.1	5.3548	9.408	9.7567	11.8122	11.8754	14.771	17.1829	19.6178	19.7655	20.3654
		0.2	5.3928	9.2977	9.6727	11.8549	11.9164	14.7645	17.2022	19.4674	19.643	20.3695
10	0	0.1	7.6343	13.8968	13.8968	16.6641	16.6641	19.6636	24.0611	27.8018	27.8018	28.5368
		0.2	7.9668	14.2971	14.2971	17.3019	17.3019	20.2299	24.9099	28.6025	28.6025	29.5013
	1	0.1	5.9604	10.6257	11.0137	13.0935	13.1022	15.8928	18.9432	21.6312	22.0709	22.5279
		0.2	6.0409	10.6112	11.0302	13.2237	13.2307	15.9447	19.0891	21.6358	22.1101	22.675
	2	0.1	5.6312	10.0026	10.4686	12.4092	12.416	15.206	17.9751	20.4726	21.013	21.3784
		0.2	5.6844	9.9443	10.4455	12.4824	12.4947	15.2074	18.0491	20.3961	20.9784	21.4375
	10	0.1	5.2936	9.2724	9.8467	11.6655	11.7014	14.4395	16.9155	19.1392	19.8242	20.091
		0.2	5.323	9.17	9.788	11.6879	11.735	14.3984	16.9245	18.9871	19.727	20.0659

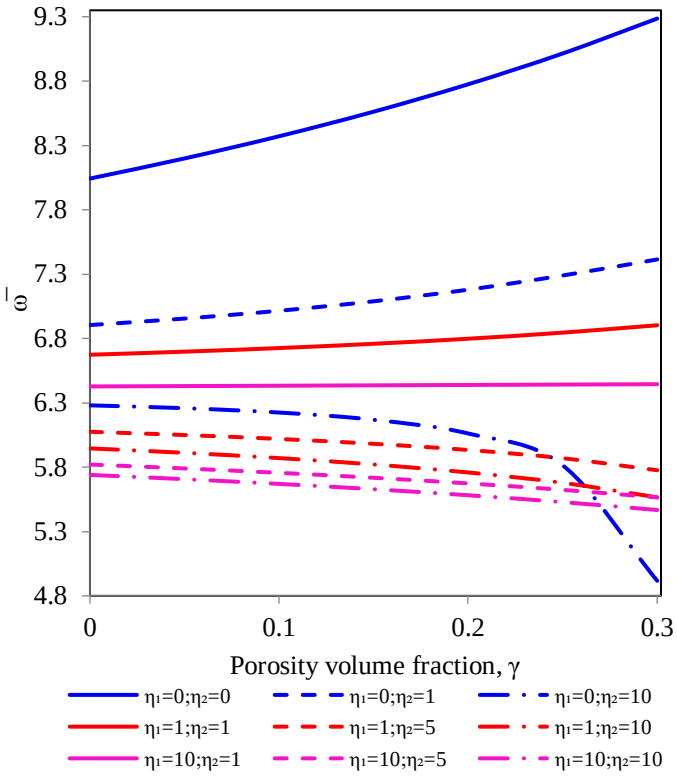

Figure. 4. The influence of porosity volume fraction, gradation indexes on the fundamental frequency of even porosity distribution, a/h=10 (a=b)

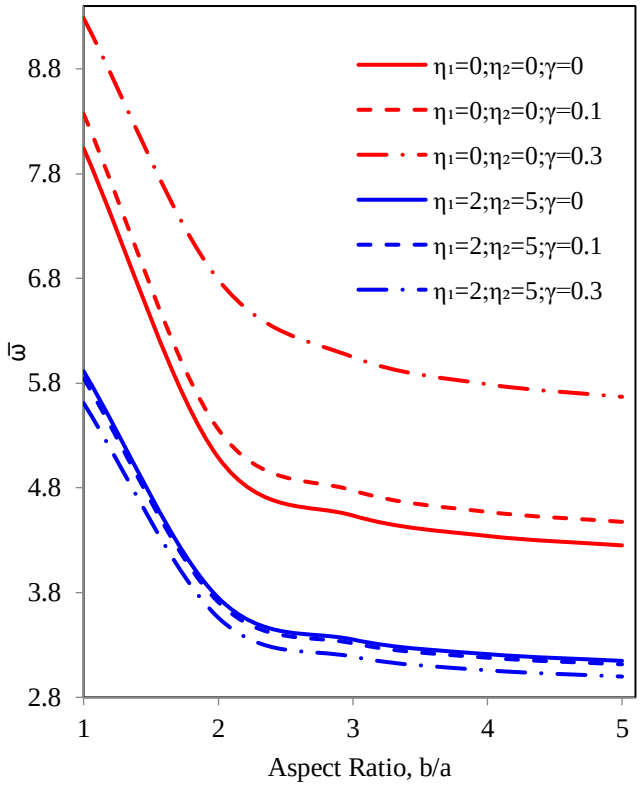

Figure. 6. The influence of aspect ratio, porosity volume fraction, gradation indexes on the fundamental frequency of even porosity distribution, a/h=10

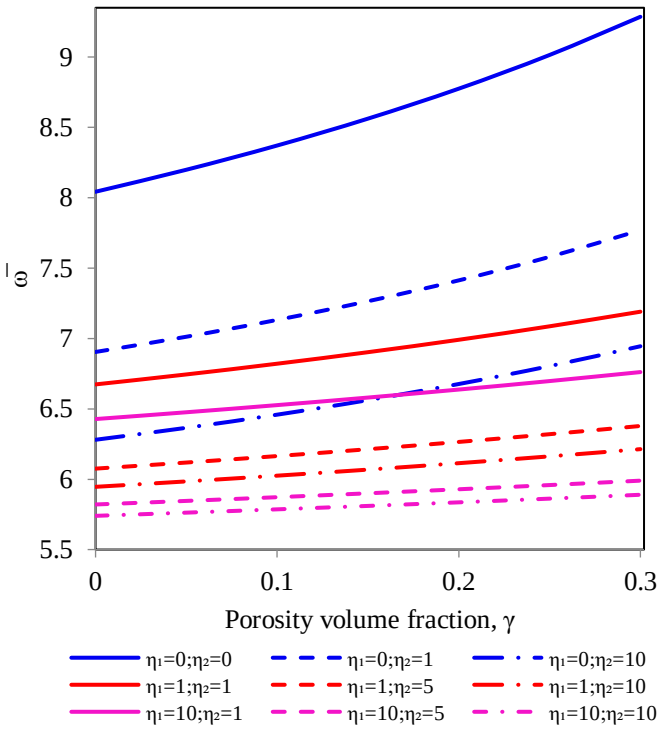

Figure. 5. The influence of porosity volume fraction, gradation indexes on the fundamental frequency of uneven porosity distribution, a/h=10 (a=b)

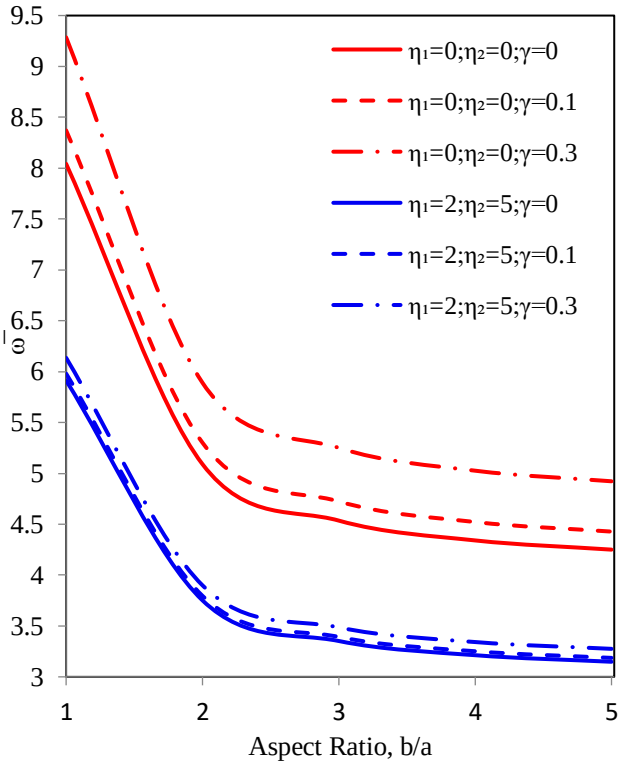

Figure. 7. The influence of aspect ratio, porosity volume fraction, gradation indexes on the fundamental frequency of uneven porosity distribution, a/h=10

References

[1] Shaw LL., 1998, The crack driving force of functionally graded materials, Journal of Materials Science Letters, doi: https://doi.org/10.1023/A:1006502026364.

[2] Valizadeh N., Natarajan S., GonZalez-Estrada O.A., Rabczuk T., Bui Q.T., Bardas P.A.S., 2013, NURBS-based finite element analysis of functionally graded plates: static bending, vibration, buckling and flutter, Composite Structures, doi: 10.1016/j.compstruct.2012.11.008.

[3] Liu P., Bui T.Q., Zhu D., Yu T.T., Wang J.W., Yin S.H., Hirose S., 2015, Buckling failure analysis of cracked functionally graded plates by a stabilized discrete shear gap extended 3-node triangular plate element, Composites Part B: Engineering, doi: https://doi.org/10.1016/j.compositesb.2015.03.036

[4] Sidda Reddy B.., Vijaya Kumar Reddy K., 2020, Flexural behavior of porous functionally graded plates using a novel higher order theory, Journal of computational applied mechanics, doi:10.22059/JCAMECH.2020.298540.488.

[5] Semsi Coskun, Jinseok Kim, Houssam Toutanji, 2019, Bending, Free Vibration, and Buckling Analysis of Functionally Graded Porous Micro-Plates Using a General Third-Order Plate Theory, Journal of composites science, doi: https://doi.org/10.3390/jcs3010015

[6] Sidda Reddy B.., Vijaya Kumar Reddy K., 2019, Thermomechanical behaviour of Functionally Graded Plates with HSDT, Journal of Computational and Applied Research in Mechanical Engineering (JCARME), doi:10.22061/jcarme.2019.5416.1674

[7] Mohammadi M., Ghayour M., Farajpour A., 2011, Analysis Of Free Vibration Sector Plate Based On Elastic Medium By Using New Version Of Differential Quadrature Method, Journal Of Simulation And Analysis Of Novel Technologies In Mechanical Engineering (Journal Of Solid Mechanics In Engineering) 3(2): 47-56.

[8] Sidda Reddy B., Suresh Kumar JEswara Reddy., C., 2011, Nonlinear bending analysis of functionally graded plates Using higher order theory, International Journal of Engineering Science and Technology (IJEST), 3 (4): 3010-3022.

[9] Sidda Reddy B., Suresh Kumar J., Eswara Reddy C., Vijaya Kumar Reddy K., 2011, Geometrically Nonlinear analysis of functionally graded material plates using higher order theory, International Journal of Engineering, Science and Technology(IJEST), 3 (1): 279-288, 2011.

[10] Sidda Reddy B., Suresh Kumar J., Eswara Reddy C., Vijaya Kumar Reddy K., 2011, Nonlinear thermal analysis of functionally graded plates using higher order theory, Innovative Systems Design and Engineering, 2 (5):1-13.

[11] Sidda Reddy B., Suresh Kumar J., Eswara Reddy C., Vijaya Kumar Reddy K., 2011, **Higher order theory for free vibration analysis of functionally graded material plates,** ARPN Journal of Engineering and Applied Sciences, 6 (10): 105-111.

[12] Mohammadi M., Farajpour A., Goodarzi M., Mohammadi H., 2013, Temperature Effect on Vibration Analysis of Annular Graphene Sheet Embedded on Visco-Pasternak Foundation, Journal of Solid Mechanics 5(3): 305-323.

[13] Safarabadi M., Mohammadi M., Farajpour A., Goodarzi M., 2015, Effect of Surface Energy on the Vibration Analysis of Rotating Nanobeam, Journal of Solid Mechanics 7(3): 299-311.

[14] Sidda Reddy B., Suresh Kumar J., Vijaya Kumar Reddy K., Buckling analysis of functionally graded material plates using higher order shear deformation theory, Journal of composites, doi: http://dx.doi.org/10.1155/2013/808764

[15] Sidda Reddy B., Suresh Kumar J., Eswara Reddy C., Vijaya Kumar Reddy K., 2014, Static Analysis of Functionally Graded Plates Using Higher-Order Shear Deformation Theory, International Journal of Applied Science and Engineering, 12 (1): 23-41.

[16] Sidda Reddy B., Suresh Kumar J., Eswara Reddy C., Vijaya Kumar Reddy K., 2014, Free Vibration Behaviour of Functionally Graded Plates Using Higher-Order Shear Deformation Theory, Journal of Applied Science and Engineering, doi: 10.6180/jase.2014.17.3.03.

[17] Sidda Reddy B., Suresh Kumar J., Eswara Reddy C., Vijaya Kumar Reddy K., 2014, Static Bending Behavior of Functionally Graded Plates Subjected to Mechanical Loading, Jordan Journal of Mechanical and Industrial Engineering, 8 (4): 169 -176.

[18] Sidda Reddy B., Suresh Kumar J., Eswara Reddy C., Vijaya Kumar Reddy K., 2015, Buckling analysis of functionally graded plates using higher order theory with thickness stretching effect, International journal of applied science and Engineering, 13 (1):19-35.

[19] Baghani M., Mohammadi M., Farajpour A., 2016, Dynamic and Stability Analysis of the Rotating Nanobeam in a Nonuniform Magnetic Field Considering the Surface Energy, International Journal of Applied Mechanics, doi:10.1142/S1758825116500484.

[20] Goodarzi M., Mohammadi M. , Khooran M., Saadi F., 2016, Thermo-Mechanical Vibration Analysis of FG Circular and Annular Nanoplate Based on the Visco-Pasternak Foundation, Journal of Solid Mechanics 8(4): 788-805.

[21] Rezaei A.S., Saidi A.R., 2015, Exact solution for free vibration of thick rectangular plates made of porous materials, Composite Structures, doi: https://doi.org/10.1016/j.compstruct.2015.08.125.

[22] Shafiei N., Mirjavadi S.S., MohaselAfshari B., Rabby S., Kazemi M., Vibration of two-dimensional imperfect functionally graded (2D-FG) porous nano-/micro-beams, Computer Methods in Applied Mechanics and Engineering, doi: https://doi.org/10.1016/j.cma.2017.05.007.

[23] Zenkour A. M., 2018, A quasi-3D refined theory for functionally graded single-layered and sandwich plates with porosities, Composite structures, doi: https://doi.org/10.1016/j.compstruct.2018.05.147

[24] Barati M.R., 2018, Vibration analysis of porous FG nanoshells with even and uneven porosity distributions using nonlocal strain gradient elasticity, Acta Mechanica, doi:https://doi.org/10.1007/s00707-017-2032-z.

[25] Jing Zhao., Kwangnam Choe., Fei Xie, Ailun Wang, Cijun Shuai and Qingshan Wang, 2018, Three-dimensional exact solution for vibration analysis of thick functionally graded porous (FGP) rectangular plates with arbitrary boundary conditions, Composites Part B: Engineering, doi: https://doi.org/10.1016/j.compositesb.2018.09.001.

[26] Barati M.R., Shahverdi H., Nonlinear vibration of nonlocal four-variable graded plates with porosities implementing homotopy perturbation and Hamil-tonian methods, Acta Mechanica. 229 (2018) 343–362. doi:https://doi.org/10.1007/s00707-017-1952-y

[27] Pinar Aydan DEMIRHAN, Vedat TASKIN, 2019, Bending and free vibration analysis of Levy-type porous functionally graded plate using state space approach, Composite Part B: Engineering 160, 661-676. doi: https://doi.org/10.1016/j.compositesb.2018.12.020

[28] Jinseok Kim, Krzysztof KamilŻur, Reddy J.N, 2019, Bending, free vibration, and buckling of modified couples stress-based functionally graded porous micro-plates, Composite structures,

209, 879-888. doi:https://doi.org/10.1016/j.compstruct.2018.11.023

[29] Chen D., Yang J., Kitipornchai S, 2019, Buckling and bending analyses of a novel functionally graded porous plate using Chebyshev-Ritz method, Archieves of Civil and Mechanical Engineering, doi: https://doi.org/10.1016/j.acme.2018.09.004

[30] Ahmed Amine Daikh, Zenkour A. M, 2019, Effect of porosity on the bending analysis of various functionally graded sandwich plates, Materials research Express, doi:https://doi.org/10.1088/2053-1591/ab0971.

[31] Slimane Merdaci, Hakima Belghoul, 2019, High-order shear theory for static analysis of functionally graded plates with porosities, C. R. Mécanique, doi: https://doi.org/10.1016/j.crme.2019.01.001

[32] Amir Farzam, Behrooz Hassani, 2019, Isogeometric analysis of in-plane functionally graded porous microplates using modified couple stress theory, Aerospace Science and Technology, doi: https://doi.org/10.1016/j.ast.2019.05.012

[33] Zamani Nejad M., Rastgoo A., Hadi A., 2014, Effect of Exponentially-Varying Properties on Displacements and Stresses in Pressurized Functionally Graded Thick Spherical Shells with Using Iterative Technique, Journal of Solid Mechanics, 6 (4): 366-377.

[34] Mohammad Zamani Nejad, Abbas Rastgoo, Amin Hadi, 2014, Exact elasto-plastic analysis of rotating disks made of functionally graded materials, International Journal of Engineering Science, doi: http://dx.doi.org/10.1016/j.ijengsci.2014.07.009

[35] Mohammad Hosseini, Mohammad Shishesaz, Khosro Naderan Tahan, Amin Hadi, 2016, Stress analysis of rotating nano-disks of variable thickness made of functionally graded materials, International Journal of Engineering Science, doi: http://dx.doi.org/10.1016/j.ijengsci.2016.09.002

[36] Mohammad Shishesaz, Mohammad Hosseini, Khosro Naderan Tahan, Amin Hadi, 2017, Analysis of functionally graded nanodisks under thermoelastic loading based on the strain gradient theory, Acta Mech, doi: 10.1007/s00707-017-1939-8

[37] Mohammad Hosseini, Mohammad Shishesaz, Amin Hadi, 2019, Thermoelastic analysis of rotating functionally graded micro/nanodisks of variable thickness, Thin-Walled Structures, doi: https://doi.org/10.1016/j.tws.2018.10.030

[38] Zeinab Mazarei and Mohammad Zamani Nejad, 2016, Thermo-Elasto-Plastic Analysis of Thick-Walled Spherical Pressure Vessels Made of Functionally Graded Materials, International Journal of Applied Mechanics, doi: 10.1142/S175882511650054X

[39] Mahboobeh Gharibi, Mohammad Zamani Nejad , Amin Hadi, 2017, Elastic analysis of functionally graded rotating thick cylindrical pressure vessels with exponentially-varying properties using power series method of Frobenius, JCAMECH, doi*:* 10.22059/jcamech.2017.233633.143

[40] Mohammad Zamani Nejad, Mehdi Jabbari and Amin Hadi, 2017, A review of functionally graded thick cylindrical and conical shells, JCAMECH, doi: 10.22059/JCAMECH.2017.247963.220

[41] Amin Hadi, Abbas Rastgoo, Nooshin Haghighipour and Azam Bolhassani, 2018, Numerical modelling of a spheroid living cell membrane under hydrostatic pressure, Journal of Statistical Mechanics: Theory and Experiment, doi: https://doi.org/10.1088/1742-5468/aad369

[42] Nejad M Z., Alamzadeh N., Hadi A., 2018, Thermoelastoplastic analysis of FGM rotating thick cylindrical pressure vessels in linear elastic-fully plastic condition, Composites Part B, doi: 10.1016/j.compositesb.2018.09.022.

[43] Behrouz Karami, Davood Shahsavari , Maziar Janghorban , Li Li, 2019, On the resonance of functionally graded nanoplates using bi-Helmholtz nonlocal strain gradient theory, International Journal of Engineering Science, doi: https://doi.org/10.1016/j.ijengsci.2019.103143

[44] Esmail Zarezadeh, Vahid Hosseini & Amin Hadi, 2019, Torsional vibration of functionally graded nano-rod under magnetic field supported by a generalized torsional foundation based on nonlocal elasticity theory, Mechanics Based Design of Structures and Machines, doi: 10.1080/15397734.2019.1642766

[45] Nemat-Alla M., 2003, Reduction of thermal stresses by developing two-dimensional functionally graded materials, Internal journal of solids and structures, doi: https://doi.org/10.1016/j.ijsolstr.2003.08.017

[46] Nemat-Alla M., 2009, Reduction of thermal stresses by composition optimization of twodimensional functionally graded materials, Acta Mechanica, doi: https://doi.org/10.1007/s00707-008-0136-1

[47] Asgari M., Akhlaghi M., 2011, Natural frequency analysis of 2D-FGM thick hollow cylinder based on three-dimensional elasticity equations, European journal of Mechanics- A/Solids, doi: https://doi.org/10.1016/j.euromechsol.2010.10.002.

[48] Ebrahimi M.J., Najafizadeh M.M., 2014, Free vibration analysis of two-dimensional functionally graded cylindrical shells, Applied mathematical modelling, doi: https://doi.org/10.1016/j.apm.2013.06.015

[49] Li L., Li X., Hu Y., 2017, Nonlinear bending of a two-dimensionally functionally graded beam, Composite Structures, doi: https://doi.org/10.1016/j.compstruct.2017.10.087

[50] Simsek M., 2015, Bi-directional functionally graded materials (BDFGMs) for free and forced vibration of Timoshenko beams with various boundary conditions, Composite Structures, doi: https://doi.org/10.1016/j.compstruct.2015.08.021.

[51] Nejad M.Z., Hadi A., 2016, Non-local analysis of free vibration of bi-directional functionally graded Euler-Bernoulli nano-beams, International journal of Engineering Science, doi: https://doi.org/10.1016/j.ijengsci.2016.04.011.

[52] Nguyen D.K., Nguyen Q.H., Tran T.T., Bui V.T., 2017, Vibration of bi-dimensional functionally graded Timoshenko beams excited by a moving load, Acta Mechanica, doi: https://doi.org/10.1007/s00707-016-1705-3

[53] Armağan Karamanlı, 2018, Free vibration analysis of two directional functionally graded beams using a third order shear deformation theory, Composite Structures doi: https://doi.org/10.1016/j.compstruct.2018.01.060.

[54] Ye Tang, Qian Ding, 2019, Nonlinear vibration analysis of a bi-directional functionally graded beam under hygro-thermal loads, Composite Structures, doi: https://doi.org/10.1016/j.compstruct.2019.111076

[55] Simsek M., 2016, Buckling of Timoshenko beams composed of two-dimensional functionally graded materials (2D-FGM) having different boundary conditions, Composite Structures, doi: https://doi.org/10.1016/j.compstruct.2016.04.034

[56] Nejad M.Z., Hadi A., Rastgoo A., 2016, Buckling analysis of arbitrary two-directional functionally graded Euler-Bernoulli nano-beams based on nonlocal elasticity theory, International Journal of Engineering science, doi: https://doi.org/10.1016/j.ijengsci.2016.03.001

[57] Karamanlı, A., 2017, Bending behaviour of two directional functionally graded sandwich beams by using a quasi-3d shear deformation theory, *Composite Structures*, doi: http://dx.doi.org/10.1016/j.compstruct.2017.04.046

[58] Lezgy-Nazargah M., 2015, Fully coupled thermo-mechanical analysis of bi-directional FGM beams using NURBS

isogeometric finite element approach, Aerospace Science and Technology, doi: https://doi.org/10.1016/j.ast.2015.05.006

[59] Apalak MK., Demirbas MD., 2016, Thermal stress analysis of in-plane two-directional functionally graded plates subjected to in-plane edge heat fluxes, Proceedings of the Institution of Mechanical Engineers, Part L: Journal of Materials: Design and Applications, doi: 10.1177/1464420716643857.

[60] Thom Van Doa, Dinh Kien Nguyenb, Nguyen Dinh Ducc,d, Duc Hong Doanc,, 2017, Tinh Quoc Bui, Analysis of bi-directional functionally graded plates by FEM and a new third-order shear deformation plate theory, Thin-Walled Structures, doi: https://doi.org/10.1016/j.tws.2017.07.022

[61] Lieu, Q.X., Lee, S., Kang, J., Lee, J., 2018, Bending and free vibration analyses of in-plane bidirectional functionally graded plates with variable thickness using isogeometric analysis, *Composite Structures*, doi: https://doi.org/10.1016/j.compstruct.2018.03.021

[62] Qui X. Lieu, Dongkyu Lee, Joowon Kang & Jaehong Lee 2018, NURBSbased modeling and analysis for free vibration and buckling problems of in-plane bi-directional functionally graded plates, Mechanics of Advanced Materials and Structures, doi: https://doi.org/10.1080/15376494.2018.1430273.

[63] Chen M., Jin G., Ma X., Zhang Y., Ye T., Liu Z., 2018, Vibration analysis for sector cylindrical shells with bi-directional functionally graded materials and elastically restrained edges, Composites Part B:Engineering, doi: 10.1016/j.compositesb.2018.08.129.

[64] Esmaeilzadeh M., Kadkhodayan M., 2019, Dynamic analysis of stiffened bi-directional functionally graded plates with porositites under a moving load by dynamic relaxation method with kinematic damping, Aerospace Science and Technology, doi: https://doi.org/10.1016/j.ast.2019.105333.

[65] Abbas Barati, Amin Hadi, Mohammad Zamani Nejad & Reza Noroozi, 2020, On vibration of bi-directional functionally graded nanobeams under magnetic field, Mechanics Based Design of Structures and Machines, doi: 10.1080/15397734.2020.1719507

[66] Abbas Barati, Mohsen Mahdavi Adeli, Amin Hadi, 2020, Static Torsion of Bi-Directional Functionally Graded Microtube Based on the Couple Stress Theory Under Magnetic Field, International Journal of Applied Mechanics, doi: 10.1142/S1758825120500210

[67] Reza Noroozi, Abbas Barati, Amin Kazemi, Saeed Norouzi and Amin Hadi, 2020, Torsional vibration analysis of bi-directional FG nano-cone with arbitrary cross-section based on nonlocal strain gradient elasticity, Advances in Nano Research**,** *doi*: http://dx.doi.org/10.12989/anr.2020.8.1.013

[68] Zhu J., Lai Z., Yin Z., Jeon J., Lee S., 2001, Fabrication of ZrO2–NiCr functionally graded material by powder metallurgy, Materials Chemistry and Physics , doi: https://doi.org/10.1016/S0254-0584(00)00355-2

[69] Timoshenko S., Woinowsky-Krieger S., 1959, Theory of platesandshells. 2nd edition. Singapore: McGraw-Hill..

[70] Vel SS., Batra RC., 2004, Three-dimensional exact solution for the vibration of functionally graded rectangular plates, Journal of sound and vibration, doi:https://doi.org/10.1016/S0022-460X(03)00412-7

[71] Hosseini-Hashemi Sh., Fadaee M., Atashipour S.R., 2011, Study on the free vibration of thick functionally graded rectangular plates according to a new exact closed-form procedure, Composite Structures, doi:10.1016/j.compstruct.2010.08.007

[72] Nguyen Van Long., Tran Huu Quoc., Tran Minh Tu., 2016, Bending and free vibration analysis of functionally graded plate using new eight-unknown shear deformation theory by finite-element method, International journal of Advanced Structural Engineering, doi: 10.1007/s40091-016-0140-y

[73] Wang WH., 2011, The elastic properties, elastic models and elastic perspectives of metallic glasses, Progress in Material Science, doi:10.1016/j.pmatsci.2011.07.001.